Fast algorithm for finding the eigenvalue distribution of very large matrices

Anthony Hams and Hans De Raedt
Institute for Theoretical Physics and Materials Science Centre, University of Groningen, Nijenborgh 4, NL-9747 AG Groningen, The Netherlands
(Received 11 April 2000)

A theoretical analysis is given of the equation of motion method, due to Alben *et al.* [Phys. Rev. B **12**, 4090 (1975)], to compute the eigenvalue distribution (density of states) of very large matrices. The salient feature of this method is that for matrices of the kind encountered in quantum physics the memory and CPU requirements of this method scale linearly with the dimension of the matrix. We derive a rigorous estimate of the statistical error, supporting earlier observations that the computational efficiency of this approach increases with the matrix size. We use this method and an imaginary-time version of it to compute the energy and specific heat of three different, exactly solvable, spin-1/2 models, and compare with the exact results to study the dependence of the statistical errors on sample and matrix size.

PACS number(s): 05.10.−a, 05.30.−d, 03.67.Lx

I. INTRODUCTION

The calculation of the distribution of eigenvalues of very large matrices is a central problem in quantum physics. This distribution determines the thermodynamic properties of the system (see below). It is directly related to the single-particle density of states (DOS) or Green's function. In a one-particle (e.g., one-electron) description, knowledge of the DOS suffices to compute the transport properties [1].

The most direct method to compute the DOS, i.e., all the eigenvalues, is to diagonalize the matrix H representing the Hamiltonian of the system. This approach has two obvious limitations: The number of operations increases as the third power of the dimension D of H, and, perhaps most importantly, the amount of memory required by state-of-the-art algorithms grows as D^2 [2,3]. This scaling behavior limits the application of this approach to matrices of dimension $D=O(10000)$, which is too small for many problems of interest. What is needed are methods that scale linearly with D.

There has been considerable interest in developing ''fast'' [i.e., $O(D)$] algorithms to compute the DOS and other similar quantities. One such algorithm and an application of it to electron motion in disordered alloy models was given by Alben *et al.* [4]. In this approach the DOS is obtained by solving the time-dependent Schrödinger equation (TDSE) of a particle moving on a lattice, followed by a Fourier transform of the retarded Green's function [4]. Using the unconditionally stable split-step fast Fourier transform method to solve the TDSE, it was shown that the eigenvalue spectrum of a particle moving in continuum space can be computed in the same manner [5]. Fast algorithms of this kind proved useful to study various aspects of localization of waves [6–8] and other one-particle problems [9–14].

Application of these ideas to quantum many-body systems triggered further development of flexible and efficient methods to solve the TDSE. Based on Suzuki's product formula approach, an unconditionally stable algorithm was developed and used to compute the time-evolution of two-dimensional $S=1/2$ Heisenberg-like models [15]. Results for the DOS of matrices of dimension $D\approx 1000000$ were reported [15]. A potentially interesting feature of these fast algorithms is that they may run very efficiently on a quantum computer [16,17].

A common feature of these fast algorithms is that they solve the TDSE for a sample of randomly chosen initial states. The efficiency of this approach as a whole relies on the hypothesis (suggested by the central limit theorem) that satisfactory accuracy can be achieved by using a small sample of initial states. Experience not only shows that this hypothesis is correct; it strongly suggests that for a fixed sample size the statistical error on physical quantities such as the energy and specific heat decreases with the dimension D of the Hilbert space [16].

In view of the general applicability of these fast algorithms to a wide variety of quantum problems, it seems warranted to analyze in detail their properties and the peculiar D dependence in particular. In Secs. II and III we recapitulate the essence of the approach. We present a rigorous estimate for the mean square error (variance) on the trace of a matrix. In Sec. IV we describe the imaginary-time version of the method. The statistical analysis of the numerical data is discussed in Sec. V. Section VI describes the model systems that are used in our numerical experiments. The algorithm used to solve the TDSE is reviewed in Sec. VII. In Sec. VIII we derive rigorous bounds on the accuracy with which all eigenvalues can be determined, and demonstrate that this accuracy decreases linearly with the time over which the TDSE is solved. The results of our numerical calculations are presented in Sec. IX, and our conclusions are given in Sec. X.

II. THEORY

The trace of a matrix A acting on a D-dimensional Hilbert space spanned by an orthonormal set of states $\{|\phi_n\rangle\}$ is given by

$$\mathrm{Tr}\,A=\sum_{n=1}^{D}\langle\phi_n|A\phi_n\rangle. \tag{1}$$

Note that according to Eq. (1) we have $\mathrm{Tr}\,1=D$. If D is very large, one might think of approximating Eq. (1) by sampling over a subset of K $(K\ll D)$ ''important'' basis vectors. The problem with this approach is that the notion ''important''

may be very model dependent. Therefore, it is better to sample in a different manner. We construct a random vector $|\psi\rangle$ by choosing D complex random numbers, $c_n \equiv f_n + ig_n$, with mean 0, for $n=1 \ldots D$, so

$$|\psi\rangle = \sum_{n=1}^{D} c_n |\phi_n\rangle, \tag{2}$$

and we calculate

$$\langle\psi|A\psi\rangle = \sum_{n,m=1}^{D} c_m^* c_n \langle\phi_m|A\phi_n\rangle. \tag{3}$$

If we now sample over S realizations of the random vectors $\{\psi\}$ and calculate the average, we obtain

$$\frac{1}{S}\sum_{p=1}^{S} \langle\psi_p|A\psi_p\rangle = \frac{1}{S}\sum_{p=1}^{S}\sum_{n,m=1}^{D} c_{m,p}^* c_{n,p} \langle\phi_m|A\phi_n\rangle. \tag{4}$$

Assuming that there is no correlation between the random numbers in different realizations, and that the random numbers $f_{n,p}$ and $g_{n,p}$ are drawn from an even and symmetric (both with respect to each variable) probability distribution (see Appendix A for more details), we have

$$\lim_{S\to\infty} \frac{1}{S}\sum_{p=1}^{S} c_{m,p}^* c_{n,p} = E(|c|^2)\,\delta_{m,n}, \tag{5}$$

where $E(\cdot)$ denotes the expectation value with respect to the probability distribution used to generate the $c_{n,p}$'s. On the right hand side of Eq. (5) the subscripts of $c_{n,p}$ have been dropped to indicate that the expectation value does not depend on n or p. It follows immediately that

$$\lim_{S\to\infty}\frac{1}{S}\sum_{p=1}^{S} \langle\psi_p|A\psi_p\rangle = E(|c|^2)\mathrm{Tr}\,A = E(|c|^2)\sum_{n=1}^{D}\langle\phi_n|A\phi_n\rangle, \tag{6}$$

showing that we can compute the trace of A by sampling over random states $\{\psi_p\}$, provided there is an efficient algorithm to calculate $\langle\psi_p|A\psi_p\rangle$ (see Sec. VII).

According to the central limit theorem, for a large but finite S, we have

$$\frac{1}{S}\sum_{p=1}^{S} c_{m,p}^* c_{n,p} = E(|c|^2)\,\delta_{m,n} + O\left(\frac{1}{\sqrt{S}}\right), \tag{7}$$

meaning that the statistical error on the trace vanishes like $1/\sqrt{S}$, which is not surprising. What is surprising is that one can prove a much stronger result as follows. Let us first normalize the $c_{n,p}$'s so that, for all p,

$$\sum_{n=1}^{D} |c_{n,p}|^2 = 1. \tag{8}$$

This innocent looking step has far reaching consequences. First we note that the normalization renders the method exact in the (rather trivial) case when the matrix A is proportional to the unit matrix. The price we pay for this is that for fixed p, the $c_{n,p}$ are now correlated, but that does not cause problems (see Appendix A). Second it follows that $E(|c|^2) = 1/D$.

Obviously the error can be written as

$$\mathrm{Tr}\,A - \frac{D}{S}\sum_{p=1}^{S}\langle\psi_p|A\psi_p\rangle = \mathrm{Tr}\,RA, \tag{9}$$

where

$$R_{m,n} \equiv \delta_{m,n} - \frac{D}{S}\sum_{p=1}^{S} c_{m,p}^* c_{n,p} \tag{10}$$

is a traceless [due to Eq. (8)] Hermitian matrix of random numbers. We put $X = \mathrm{Tr}\,RA$, and compute $E(|X|^2)$. The result for the general case can be found in Appendix A. For a uniform distribution of the $c_{n,p}$'s on the hypersphere defined by $\Sigma_{n=1}^{D}|c_{n,p}|^2 = 1$, the expression simplifies considerably, and we find

$$E(|\mathrm{Tr}\,RA|^2) = \frac{D\,\mathrm{Tr}\,A^\dagger A - |\mathrm{Tr}\,A|^2}{S(D+1)}, \tag{11}$$

an exact expression for the variance in terms of the sample size S, the dimension D of the matrix A, and the (unknown) constants $\mathrm{Tr}\,A^\dagger A$, and $|\mathrm{Tr}\,A|$.

Invoking a generalization of Markov's inequality [18]

$$\mathbf{P}(|X|^2 \geqslant a) \leqslant \frac{E(|X|^2)}{a},\ \forall\, a>0, \tag{12}$$

where $\mathbf{P}(Q)$ denotes the probability for the statement Q to be true. We find that the probability that $|\mathrm{Tr}\,RA|^2$ exceeds a fraction a of $|\mathrm{Tr}\,A|^2$ is bounded by

$$\mathbf{P}\left(\frac{|\mathrm{Tr}\,RA|^2}{|\mathrm{Tr}\,A|^2} \geqslant a\right) \leqslant \frac{1}{a\,S\,(D+1)}\,\frac{D\,\mathrm{Tr}\,A^\dagger A - |\mathrm{Tr}\,A|^2}{|\mathrm{Tr}\,A|^2};$$

$$\forall\, a>0, \tag{13}$$

or, in other words, the relative statistical error e_A on the estimator of the trace of A is given by

$$e_A \equiv \sqrt{\frac{D\,\mathrm{Tr}\,A^\dagger A - |\mathrm{Tr}\,A|^2}{S(D+1)|\mathrm{Tr}A|^2}} \tag{14}$$

if $|\mathrm{Tr}\,A|>0$. We see that $e_A=0$ if A is proportional to a unit matrix. From Eq. (14) it follows that, in general, we may expect e_A to vanish with the square root of SD. The prefactor is a measure for the relative spread of the eigenvalues of A, and is obviously model dependent. The dependence of e_A on S, D, and the spectrum of A is corroborated by the numerical results presented below.

It is also of interest to examine the effect of *not* normalizing the $c_{n,p}$'s. A calculation similar to the one that led to the above results yields

$$e_A = \sqrt{\frac{\mathrm{Tr}\,A^\dagger A}{S|\mathrm{Tr}\,A|^2}}. \tag{15}$$

Clearly, this bound is less sharp and does not vanish if A is proportional to a unit matrix.

III. REAL-TIME METHOD

The distribution of eigenvalues or DOS of a quantum system is defined as

$$\mathcal{D}(\epsilon)=\sum_{n=1}^{D}\delta(\epsilon-E_n)=\frac{1}{2\pi}\int_{-\infty}^{\infty}e^{it\epsilon}\,\mathrm{Tr}\,e^{-itH}\,dt, \quad (16)$$

where H is the Hamiltonian of the system and n runs over all the eigenvalues of H. The DOS contains all the physical information about the equilibrium properties of the system. For instance the partition function, the energy, and the heat capacity are given by

$$Z=\int_{-\infty}^{\infty}d\epsilon\,\mathcal{D}(\epsilon)\,e^{-\beta\epsilon}, \quad (17)$$

$$E=\frac{1}{Z}\int_{-\infty}^{\infty}d\epsilon\,\epsilon\,\mathcal{D}(\epsilon)\,e^{-\beta\epsilon}, \quad (18)$$

$$C=\beta^2\left(\frac{1}{Z}\int_{-\infty}^{\infty}d\epsilon\,\epsilon^2\,\mathcal{D}(\epsilon)\,e^{-\beta\epsilon}-E^2\right), \quad (19)$$

respectively. Here $\beta=1/k_BT$ and k_B is Boltzmann's constant (we put $k_B=1$ and $\hbar=1$ from now on).

As explained above, the trace in integral (16) can be estimated by sampling over random vectors. For the statistical error analysis discussed below it is convenient to define a DOS per sample by

$$d_p(\epsilon)\equiv\frac{1}{2\pi}\int_{-\infty}^{\infty}e^{it\epsilon}\langle\psi_p|e^{-itH}\psi_p\rangle dt, \quad (20)$$

where the subscript p labels the particular realization of the random state $|\psi_p\rangle$. The DOS is then given by

$$\mathcal{D}(\epsilon)=\lim_{S\to\infty}\frac{1}{S}\sum_{p=1}^{S}d_p(\epsilon). \quad (21)$$

Schematically the algorithm to compute $d_p(\epsilon)$ consists of the following steps: (1) Generate a random state $|\psi_p(0)\rangle$, and set $t=0$. (2) Copy this state to $|\psi_p(t)\rangle$. (3) Calculate $\langle\psi_p(0)|\psi_p(t)\rangle$ and store the result. (4) Solve the TDSE for a small time step τ, replacing $|\psi_p(t)\rangle$ by $|\psi_p(t+\tau)\rangle$ (see Sec. VII for model specific details). (5) Repeat N times from step (3). (6) Perform a Fourier transform on the tabulated result, and store $d_p(\epsilon)$.

In practice the Fourier transform in Eq. (16) is performed by the fast Fourier transform (FFT). We use a Gaussian window to account for the finite time τN used in the numerical time integration of the TDSE. The number of time step N determines the accuracy with which the eigenvalues can be computed. In Sec. VIII we prove that this systematic error in the eigenvalues vanishes as $1/\tau N$.

Since for any reasonable physical system (or finite matrix) the smallest eigenvalue E_0 is finite, for all practical purposes $d_p(\epsilon)=0$ for $\epsilon<\epsilon_0<E_0$. The value of ϵ_0 is easily determined by examination of the bottom of spectrum. To compute Z, E, or C, we simply replace the interval $[-\infty,+\infty]$ by $[\epsilon_0,+\infty]$.

IV. IMAGINARY-TIME METHOD

The real-time approach has the advantage that it yields information on all eigenvalues and can be used to compute both dynamic and static properties without suffering from numerical instabilities. However for the computation of the thermodynamic properties, the imaginary-time version is more efficient. We will use the imaginary-time method as an independent check on the results obtained by the real-time algorithm.

Repeating the steps that lead to Eq. (17), we find

$$Z=\mathrm{Tr}\exp(-\beta H)=\lim_{S\to\infty}\frac{1}{S}\sum_{p=1}^{S}\langle\psi_p|\exp(-\beta H)\psi_p\rangle, \quad (22)$$

with similar expressions for E and C.

Furthermore we have

$$\langle\psi_p|H^ne^{-\beta H}\psi_p\rangle=\langle e^{-\beta H/2}\psi_p|H^ne^{-\beta H/2}\psi_p\rangle, \quad (23)$$

assuming H is Hermitian. Therefore we only need to propagate the random state for an imaginary time $\beta/2$ instead of β. Furthermore we do not need to perform a FFT. Disregarding these minor differences, the algorithm is the same as in the real-time case with τ replaced by $-i\tau$.

V. ERROR ANALYSIS

Estimating the statistical error on the partition function Z is easy because it depends linearly on the trace of the (imaginary) time evolution operator. However, the error on E and C depends on this trace in a more complicated manner, and this fact has to be taken into account.

First we define

$$z_p\equiv\int_{\epsilon_0}^{\infty}d\epsilon\,d_p(\epsilon)\,e^{-\beta\epsilon}, \quad (24)$$

$$h_p\equiv\int_{\epsilon_0}^{\infty}d\epsilon\,d_p(\epsilon)\,\epsilon\,e^{-\beta\epsilon}, \quad (25)$$

$$w_p\equiv\int_{\epsilon_0}^{\infty}d\epsilon\,d_p(\epsilon)\,\epsilon^2\,e^{-\beta\epsilon} \quad (26)$$

for the real-time method, and

$$z_p\equiv\langle\psi_p|e^{-\beta H}\psi_p\rangle, \quad (27)$$

$$h_p\equiv\langle\psi_p|He^{-\beta H}\psi_p\rangle, \quad (28)$$

$$w_p\equiv\langle\psi_p|H^2e^{-\beta H}\psi_p\rangle \quad (29)$$

for the imaginary-time method. For each value of β we generate the data $\{z_p\}$, $\{h_p\}$, and $\{w_p\}$, for $p=1,\ldots,S$. For both cases we have

$$Z = \lim_{S\to\infty} \overline{z}, \tag{30}$$

$$E = \lim_{S\to\infty} \frac{\overline{h}}{\overline{z}}, \tag{31}$$

$$C = \lim_{S\to\infty} \beta^2 \left(\frac{\overline{w}}{\overline{z}} - \frac{\overline{h^2}}{\overline{z^2}} \right), \tag{32}$$

where $\overline{x} \equiv S^{-1}\Sigma_{p=1}^{S} x_p$. The standard deviations on $\overline{z}$, $\overline{h}$, and $\overline{w}$ are given by

$$\delta z = \sqrt{\frac{\mathrm{var}(z)}{S-1}}, \tag{33}$$

$$\delta h = \sqrt{\frac{\mathrm{var}(h)}{S-1}}, \tag{34}$$

$$\delta w = \sqrt{\frac{\mathrm{var}(w)}{S-1}}, \tag{35}$$

where $\mathrm{var}(x) \equiv \overline{x^2} - \overline{x}^2$ denotes the variance on the data $\{x_p\}$. However, the sets of data $\{z_p\}$, $\{h_p\}$, and $\{w_p\}$ are correlated, since they are calculated from the same set $\{|\psi_p\rangle\}$. These correlations in the data are accounted for by calculating the covariance matrix $\underline{M_{k,l}}$ $(k,l=1,\ldots,3)$, the elements of which are given by $x_k x_l - x_k\, x_l$, where $\{x_1\}$, $\{x_2\}$, and $\{x_3\}$ are a shorthand for $\{z_p\}$, $\{h_p\}$, and $\{w_p\}$, respectively. The estimates for the errors in Z, E, and C are given by

$$\delta Z^2 = \frac{1}{S-1}\,\delta z^2, \tag{36}$$

$$\delta E^2 = \frac{1}{S-1} \sum_{k,l=1}^{3} M_{k,l} \frac{d\overline{E}}{d\overline{x_k}} \frac{d\overline{E}}{d\overline{x_l}}, \tag{37}$$

$$\delta C^2 = \frac{1}{S-1} \sum_{k,l=1}^{3} M_{k,l} \frac{d\overline{C}}{d\overline{x_k}} \frac{d\overline{C}}{d\overline{x_l}}, \tag{38}$$

where $\overline{E} = \overline{h}/\overline{z}$ and and $\overline{C} = \beta^2(\overline{w}/\overline{z} - \overline{h^2}/\overline{z^2})$.

VI. EXACTLY SOLVABLE SPIN 1/2 MODELS

The most direct way to assess the validity of the approach described above is to carry out numerical experiments on exactly solvable models. In this paper we consider three different exactly solvable models, two spin-1/2 chains and a mean-field spin-1/2 model. The former have a complicated spectrum, the latter has a highly degenerate eigenvalue distribution. These spin models differ from those studied elsewhere [15,16], in that they belong to the class of integrable systems.

A. Spin chains

Open spin chains of L sites described by the Hamiltonian

$$H = -J \sum_{i=1}^{L-1} (\sigma_i^x \sigma_{i+1}^x + \Delta \sigma_i^y \sigma_{i+1}^y) - h \sum_{i=1}^{L} \sigma_i^z \tag{39}$$

—where σ_i^x, σ_i^y, and σ_i^z denote the Pauli matrices, and J, Δ, and h are model parameters—can be solved exactly. They can be reduced to diagonal form by means of the Jordan-Wigner transformation [19]. We have

$$H = \sum_{i,j=1}^{L} \left[c_i^\dagger A_{i,j} c_j + \frac{1}{2}(c_i^\dagger B_{i,j} c_j^\dagger + c_j B_{j,i}^* c_i) \right] + hL, \tag{40}$$

where $c_i^\dagger$ and c_i are spinless fermion operators and

$$A_{i,j} = -J(1+\Delta)(\delta_{i,j-1} + \delta_{i-1,j}) - 2h\,\delta_{i,j}, \tag{41}$$

$$B_{i,j} = -J(1-\Delta)(\delta_{i,j-1} - \delta_{i-1,j}) \tag{42}$$

are $L \times L$ matrices. By further canonical transformation, this Hamiltonian can be written as

$$H = \sum_{k=1}^{L} \Lambda_k \left(n_k - \frac{1}{2} \right) + \frac{1}{2}\mathrm{Tr}\,A + hL, \tag{43}$$

where n_k is the number operator of state k, and the Λ_k's are given by the solution of the eigenvalue equation

$$(A-B)(A+B)\,\phi_k = \Lambda_k^2\,\phi_k. \tag{44}$$

In the general case this eigenvalue problem of the $L \times L$ Hermitian matrix $(A-B)(A+B)$ is most easily solved numerically. In the present paper we confine ourselves to two limiting cases: the XY model $(\Delta = 1)$, and the Ising model in a transverse field $(\Delta = 0)$.

B. Mean-field model

The Hamiltonian of the mean-field model reads

$$H = -\frac{J}{L} \sum_{i>j=1}^{L} \vec{\sigma}_i \cdot \vec{\sigma}_j - h \sum_{i=1}^{L} \sigma_i^z, \tag{45}$$

and can be rewritten as

$$H = -2\frac{J}{L}\vec{S}\cdot\vec{S} - 2hS^z + \frac{3}{2}J, \tag{46}$$

with

$$\vec{S} = \frac{1}{2} \sum_{i=1}^{L} \vec{\sigma}_i. \tag{47}$$

The single spin-$L/2$ Hamiltonian has eigenvalues

$$E_{l,m} = -2Jl(l+1)/L - 2hm + \frac{3}{2}J, \tag{48}$$

with degeneracy

$$n_{l,m}=\frac{2l+1}{L/2+l+1}\binom{L}{L/2-l}. \tag{49}$$

This rather trivial model serves as a test for the case of highly degenerate eigenvalues.

VII. TIME EVOLUTION

For the approach outlined in Secs. III and IV to be of practical use, it is necessary that the matrix elements of the exponential of H can be calculated efficiently. The purpose of this section is to describe how this can be done.

The general form of the Hamiltonians of the models we study is

$$H=-\sum_{i,j=1}^{L}\sum_{\alpha=x,y,z}J_{i,j}^{\alpha}\sigma_i^{\alpha}\sigma_j^{\alpha}-\sum_{i=1}^{L}\sum_{\alpha=x,y,z}h_i^{\alpha}\sigma_i^{\alpha}, \tag{50}$$

where the first sum runs over all pairs P of spins, σ_i^{α} ($\alpha=x,y,z$) denotes the αth component of the spin-1/2 operator representing the ith spin. For both methods, we have to calculate the evolution of a random state, i.e., $U(\tau)|\psi\rangle \equiv \exp(-i\tau H)|\psi\rangle$ or $U(\tau)|\psi\rangle \equiv \exp(-\tau H)|\psi\rangle$ for the real and imaginary time methods, respectively. We will discuss the real-time case only; the imaginary-time problem can be solved in the same manner.

Using the semigroup property $U(t_1)U(t_2)=U(t_1+t_2)$, we can write $U(t)=U(\tau)^m$ where $t=m\tau$. Then the main step is to replace $U(\tau)$ by a symmetrized product-formula approximation [20]. For the case at hand it is expedient to take

$$U(\tau)\approx\tilde{U}(\tau)\equiv e^{-i\tau H_z/2}e^{-i\tau H_y/2}e^{-i\tau H_x}e^{-i\tau H_y/2}e^{-i\tau H_z/2}, \tag{51}$$

where

$$H_{\alpha}=-\sum_{i,j=1}^{L}J_{i,j}^{\alpha}\sigma_i^{\alpha}\sigma_j^{\alpha}-\sum_{i=1}^{L}h_i^{\alpha}\sigma_i^{\alpha}, \quad \alpha=x,y,z. \tag{52}$$

Other decompositions [15,21] work equally well, but are somewhat less efficient for the cases at hand. In the real-time approach $\tilde{U}(\tau)$ is unitary, and hence the method is unconditionally stable [20] (also the imaginary-time method can be made unconditionally stable). It can be shown that $\|U(\tau)-\tilde{U}(\tau)\|\leqslant s\tau^3$ ($s>0$ a constant) [22], implying that the algorithm is correct to second order in the time step τ [20]. Usually it is not difficult to choose τ so small that for all practical purposes the results obtained can be considered as being ''exact.'' Moreover, if necessary, $\tilde{U}(\tau)$ can be used as a building block to construct higher-order algorithms [23–26]. In Appendix B we will derive bounds on the error in the eigenvalues when they are calculated using a symmetric product formula.

As basis states $\{|\phi_n\rangle\}$ we take the direct product of the eigenvectors of the S_i^z (i.e., spin-up $|\uparrow_i\rangle$ and spin-down $|\downarrow_i\rangle$). In this basis, $e^{-i\tau H_z/2}$ changes the input state by altering the phase of each of the basis vectors. As H_z is a sum of pair interactions, it is trivial to rewrite this operation as a direct product of 4×4 diagonal matrices (containing the interaction-controlled phase shifts) and 4×4 unit matrices. Still working in the same representation, the action of $e^{-i\tau H_y/2}$ can be written in a similar manner, but the matrices that contain the interaction-controlled phase-shift have to be replaced by nondiagonal matrices. Although this does not present a real problem, it is more efficient and systematic to proceed as follows. Let us denote by $X(Y)$ the rotation by $\pi/2$ of each spin about the $x(y)$ axis. As

$$e^{-i\tau H_y/2}=XX^{\dagger}e^{-i\tau H_y/2}XX^{\dagger}=Xe^{-i\tau H_z'/2}X^{\dagger}, \tag{53}$$

it is clear that the action of $e^{-i\tau H_y/2}$ can be computed by applying to each spin, the inverse of X followed by an interaction-controlled phase-shift and X itself. The prime in Eq. (53) indicates that $J_{i,j}^z$ and h_i^z in H_z have to be replaced by $J_{i,j}^y$ and h_i^y respectively. A similar procedure is used to compute the action of $e^{-i\tau H_x}$. We only have to replace X by Y.

VIII. ACCURACY OF THE COMPUTED EIGENVALUES

First we consider the problem of how to choose the number of time steps N to obtain the DOS with acceptable accuracy. According to the Nyquist sampling theorem employing a sampling interval $\Delta t=\pi/\max_i|E_i|$ is sufficient to cover the full range of eigenvalues. On the other hand, the time step also determines the accuracy of the approximation $\tilde{U}(\tau)$. Let us call the maximum value of τ which gives satisfactory accuracy τ_0 (for the imaginary-time method, this is the only parameter). For the examples treated here $\tau_0<\Delta t$), implying that we have to use more steps to solve the TDSE than we actually use to compute the FFT. Eigenvalues that differ less than $\Delta\epsilon=\pi/N\Delta t$ cannot be identified properly. However, since $\Delta\epsilon\propto N^{-1}$ we only have to extend the length of the calculation by a factor of 2 to increase the resolution by the same factor.

At first glance the above reasoning may seem to be a little optimistic. It apparently overlooks the fact that if we integrate the TDSE over longer and longer times the error on the wave function also increases (although it remains bounded because of the unconditional stability of the product formula algorithm). In fact it has been shown that, in general [20],

$$\left\|e^{-itH}|\psi(0)\rangle-\tilde{U}^m(\tau)|\psi(0)\rangle\right\|\leqslant c\tau^2t, \tag{54}$$

where $t=m\tau$, suggesting that the loss in accuracy on the wave function may well compensate for the gain in resolution that we obtain by using more data in the Fourier transform. Fortunately this argument does not apply when we want to determine the eigenvalues as we now show. As before, we will discuss the real-time algorithm only because the same reasoning (but different mathematical proofs) holds for the imaginary-time case.

Consider the time-step operator (52). Using the fact that any unitary matrix can be written as the matrix exponential of a Hermitian matrix, we can write

$$\tilde{U}(\tau)=e^{-i\tau H_z/2}e^{-i\tau H_y/2}e^{-i\tau H_x}e^{-i\tau H_y/2}e^{-i\tau H_z/2}\equiv e^{-i\tau\tilde{H}(\tau)}. \tag{55}$$

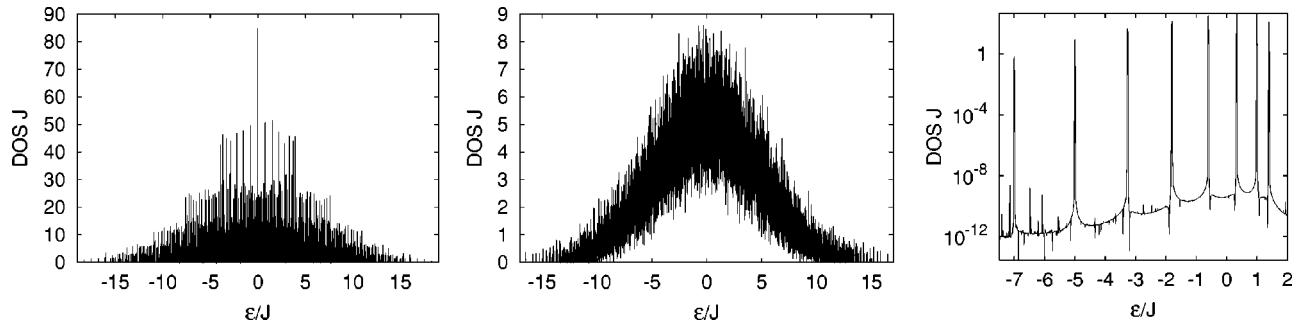

FIG. 1. The density of states (DOS) as obtained from the real-time algorithm for spin chains of length $L=15$ and for $S=20$ random initial states. Left: XY model; middle: Ising model in a transverse field; right: mean-field model. For the mean-field model a logarithmic scale was used to show the highly degenerate spectrum more clearly.

It is clear that in practice the real-time method yields the spectrum of $\tilde{H}(\tau)$, not the one of H. Therefore the relevant question is: How much do the spectra of $\tilde{H}(\tau)$ and H differ? In Appendix B we give a rigorous proof that the difference between the eigenvalues of $\tilde{H}(\tau)$ and H vanishes as τ^2. In other words the value of m (or $t=m\tau$) has no effect whatsoever on the accuracy with which the spectrum can be determined. Therefore, the final conclusion is that the error in the eigenvalues vanishes as τ^2/N where N is the number of data points used in the Fourier transform of $\mathrm{Tr}\, e^{-it\tilde{H}(\tau)}$.

IX. RESULTS

We write our results in units of J and take $h=0$, except for the Ising model in a transverse field, where we take $h=0.75J$. The random numbers $c_{n,p}$ are generated such that the Eqs. (A3) and (A4) are satisfied. We use two different techniques to generate these random numbers.

(1) A uniform random number generator produces $\{f_{n,p}\}$ and $\{g_{n,p}\}$ with $-1\leqslant f_{n,p},g_{n,p}\leqslant 1$. We then normalize the vector [see Eq. (8)].

(2) $c_{n,p}$'s are obtained from a two-variable (real and imaginary part) Gaussian random number generator and the resulting vector is normalized.

Both methods satisfy the basic requirements Eqs. (A3) and (A4) but because the first samples points out of a $2D$-dimensional hypercube and subsequently projects the vector onto a sphere, the points are not distributed uniformly over the surface of the unit hypersphere. The second method is known to generate numbers which are distributed uniformly over the hypersurface. Although the first method does not satisfy all the mathematical conditions that lead to error (14), our numerical experiments with both generators give identical results, within statistical errors of course. Also, within the statistical errors, the results from the imaginary and real-time algorithm are the same. Therefore, we only show some representative results as obtained from the real-time algorithm.

In Fig. 1 we show a typical result for the DOS $D(\epsilon)$ of the XY model, the Ising model in a transverse field, and the mean-field model, all with $L=15$ spins and using $S=20$ samples. Because of the very high degeneracy we plotted the DOS for the mean-field model on a logarithmic scale.

In Fig. 2 we show the relative error $\delta Z/Z$ based on Eq. (36) for the three models of various size, as obtained from the simulation (symbols). For these figures we used the imaginary-time algorithm, because then the statistical error can be related to e_A directly [see Eq. (14), with $A=\exp(-\beta H)$]. The theoretical results (lines) for the error estimate, obtained by a direct exact numerical evaluation of Eq. (14) are shown as well. We conclude that for all systems, lattice sizes, and temperatures there is very good agreement between numerical experiment and theory.

Results for the energy E and specific heat C are presented in Fig. 3 the (XY model), 4 (the Ising model in a transverse field), and 5 (the mean-field model). The solid lines represent the exact result for the case shown. Simulation data as obtained from $S=5$ and 20 samples are represented by symbols, and the estimates of the statistical error by error bars. We see that the data are in excellent agreement with the

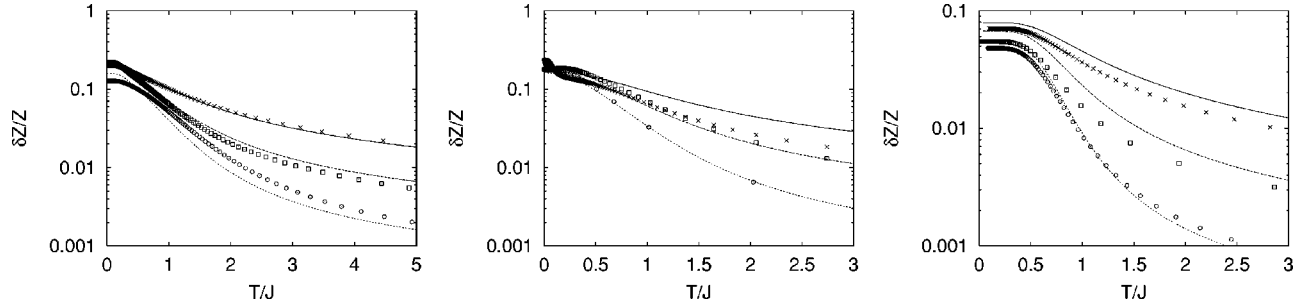

FIG. 2. The relative error $\delta Z/Z$ [see Eq. (36)] on a logarithmic scale as a function of temperature $T\equiv 1/\beta$ and for various system sizes. Left: XY model; middle: Ising model in a transverse field; right: mean-field model. Solid lines: e_A [with $A=e^{-\beta H}$; see Eq. (14)] for $L=6$; dashed lines: e_A for $L=10$; dash-dotted line: e_A for $L=15$. Crosses: simulation data for $S=20$ and $L=6$; squares: simulation data for $S=20$ and $L=10$; circles: simulation data for $S=20$ and $L=15$.

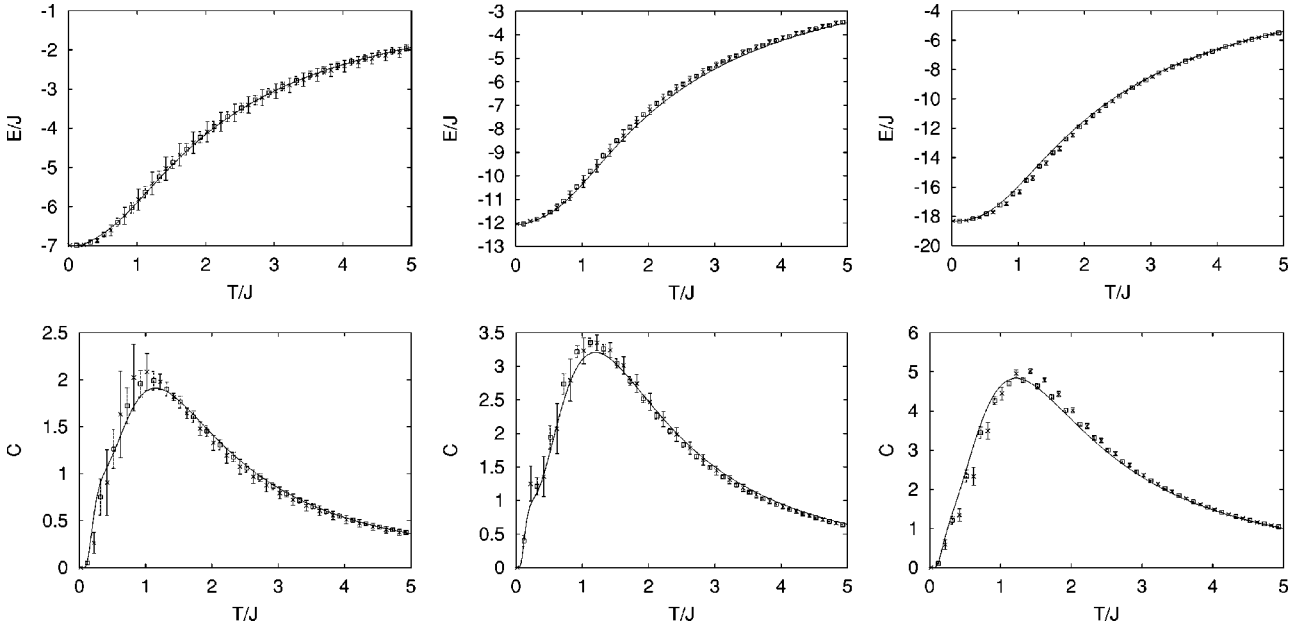

FIG. 3. Energy (top) and specific heat (bottom) of the XY model [see Eq. (39)], with $\Delta=1$ and $h=0$. Left: $L=6$; middle: $L=10$; right: $L=15$. Solid lines: exact result; crosses: simulation data using $S=5$ samples; squares: simulation data using $S=20$ samples. Error bars: One standard deviation.

exact results and, equally important, the estimate for the error captures the deviation from the exact result very well. We also see that in general the error decreases with the system size. Both the imaginary- and real-time methods seem to work very well, yielding accurate results for the energy and specific heat of quantum spin systems with modest amounts of computational effort.

X. CONCLUSIONS

The theoretical analysis presented in this paper gives a solid justification of the remarkable efficiency of the real-time equation-of-motion method for computing the distribution of all eigenvalues of very large matrices. The real-time method can be used whenever the more conventional, Lanczos-like, sparse-matrix techniques can be applied: Memory and CPU requirements for each iteration (time-step) are roughly the same (depending on the actual implementation) for both approaches.

We do not recommend using the real-time method if one is interested in the smallest (or largest) eigenvalue only. Then the Lanczos method is computationally more efficient because it needs less iterations (time steps) than the real-time approach. However, if one needs information about all ei-

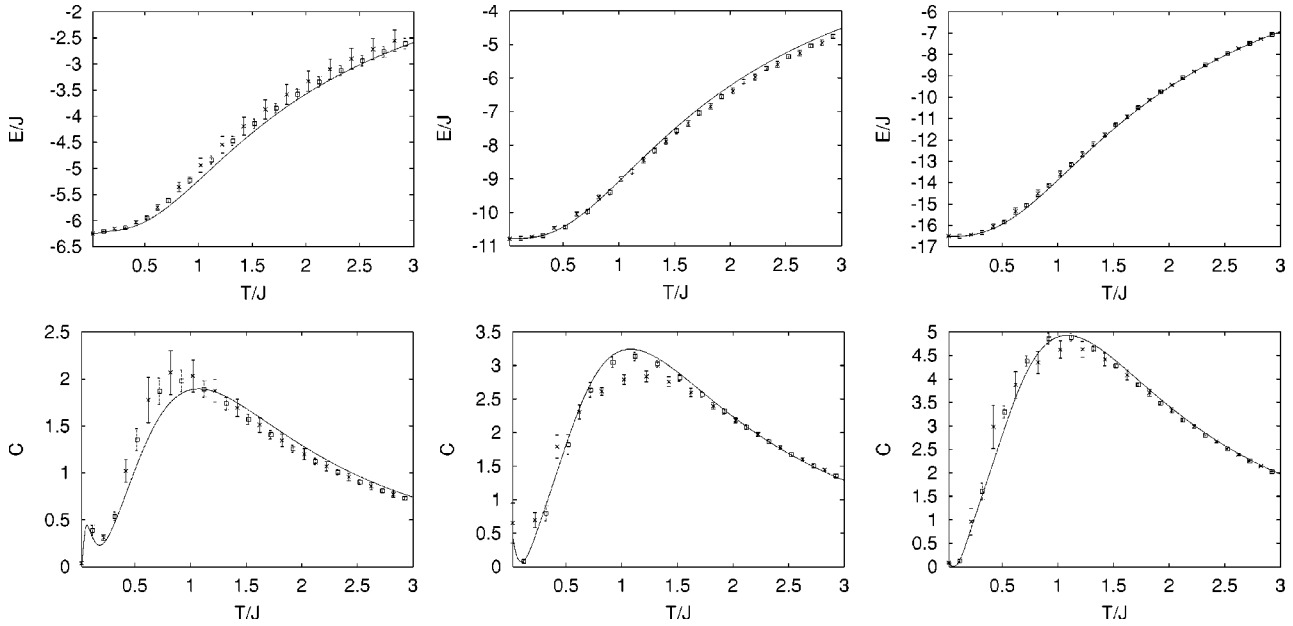

FIG. 4. Energy (top) and specific heat (bottom) of the Ising model in a transverse field [see Eq. (39)] with $\Delta=0$ and $h=0.75J$. Left: $L=6$; middle: $L=10$; right: $L=15$. Solid lines; exact result; crosses: simulation data using $S=5$ samples; squares: simulation data using $S=20$ samples. Error bars: one standard deviation.

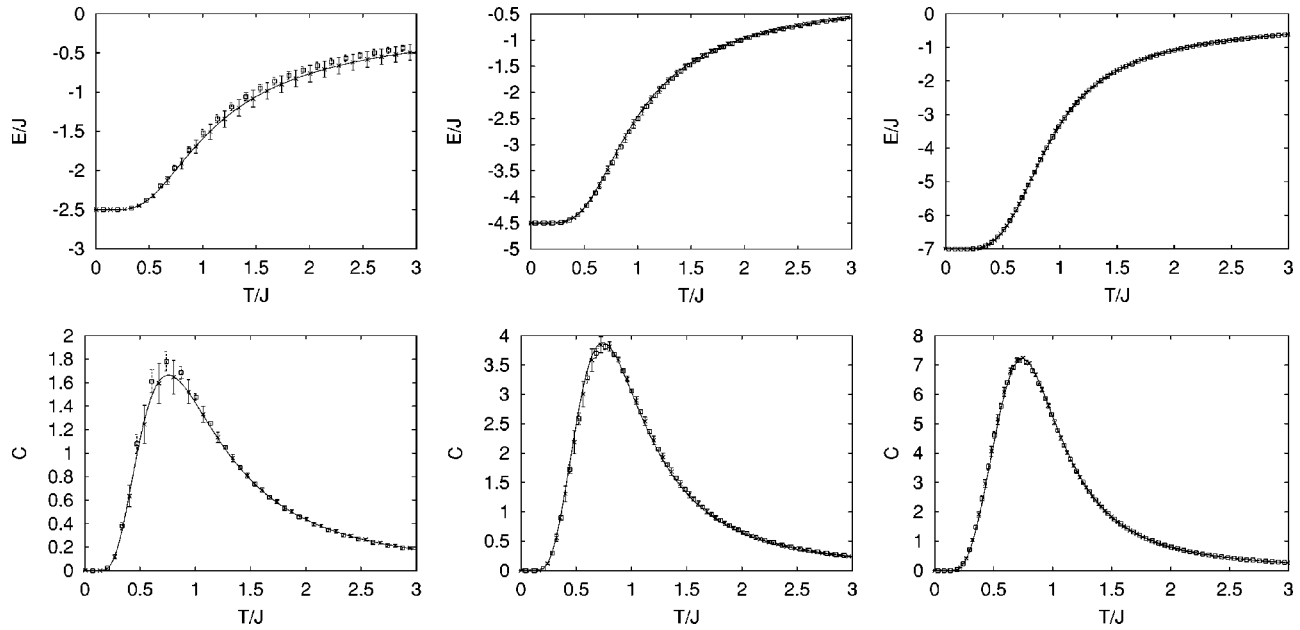

FIG. 5. Energy (top) and specific heat (bottom) of the mean-field model [see Eq. (45)] with $h=0$. Left: $L=6$; middle: $L=10$; right: $L=15$. Solid lines: exact result; crosses: simulation data using $S=5$ samples; squares: simulation data using $S=20$ samples. Error bars: one standard deviation.

genvalues and direct diagonalization is not possible (because of memory/CPU time) there is as yet no alternative to the real-time method. The matrices used in this example (up to 32768×32768) are not representative in this respect: The real-time method has been used to compute the distribution of eigenvalues for matrices of dimension 16777216×16777216 [15].

Once the eigenvalue distribution is known the thermodynamic quantities directly follow. However, if one is interested in the accurate determination of the temperature dependence of thermodynamic (and static correlation functions) properties but not in the eigenvalue distribution itself, the imaginary-time method is by far the most efficient method to compute these quantities. For instance the calculation of the thermodynamic properties for $\beta J=0,\ldots,10$ of a 15-site spin-1/2 system (i.e. implicitly solving the full 32768×32768 eigenvalue problem) takes 1410 sec per sample on a Mobile Pentium III 500 MHz system.

Finally we remark that although we used quantum-spin models to illustrate various aspects, there is nothing in the real or imaginary-time method that is specific to the models used. The only requirement for these methods to be useful in practice is that the matrix is sparse and (very) large.

ACKNOWLEDGMENTS

Support from the Dutch ''Stichting Nationale Computer Faciliteiten (NCF)'' and the Dutch ''Stichting voor Fundamenteel Onderzoek der Materie (FOM)'' is gratefully acknowledged.

APPENDIX A: EXPECTATION VALUE CALCULATION

In this Appendix we calculate the expectation value of the error squared, as defined in Sec. II. By definition we have

$$E(|\mathrm{Tr}\,RA|^2)=E\left(\left|\frac{1}{S}\sum_{p=1}^{S}\sum_{m,n=1}^{D}(\delta_{m,n}-D\,c^*_{m,p}c_{n,p})A_{m,n}\right|^2\right)$$
$$=\frac{1}{S^2}\sum_{p,p'=1}^{S}\sum_{k,l,m,n=1}^{D}(\delta_{k,l}\delta_{m,n}-D\,\delta_{k,l}E(c^*_{m,p}c_{n,p})-D\,\delta_{m,n}E(c_{k,p'}c^*_{l,p'})$$
$$+D^2E(c^*_{m,p}c_{n,p}c_{k,p'}c^*_{l,p'}))A^*_{k,l}A_{m,n}, \tag{A1}$$

where p and p' label the realization of the random numbers $c_{n,p}\equiv f_{n,p}+ig_{n,p}$.

First we assume that different realizations $p\neq p'$ are independent implying that

$$E(c^*_{m,p}c_{n,p}c_{k,p'}c^*_{l,p'})_{p\neq p'}=E(c^*_{m,p}c_{n,p})E(c_{k,p'}c^*_{l,p'}). \tag{A2}$$

Second we assume that the random numbers are drawn from a probability distribution that is an even function of each variable,

$$P(f_{1,p},g_{1,p},f_{2,p},g_{2,p},\ldots,f_{k,p},g_{k,p},\ldots,f_{D,p},g_{D,p}) = P(f_{1,p},g_{1,p},f_{2,p},g_{2,p},\ldots,-f_{k,p},g_{k,p},\ldots,f_{D,p},g_{D,p}) = P(f_{1,p},g_{1,p},f_{2,p},g_{2,p},\ldots,f_{k,p},-g_{k,p},\ldots,f_{D,p},g_{D,p}), \quad \text{(A3)}$$

and symmetric under interchange of any two variables,

$$P(f_{1,p},g_{1,p},\ldots,f_{i,p},g_{i,p},\ldots,f_{j,p},g_{j,p},\ldots,f_{D,p},g_{D,p}) = P(f_{1,p},g_{1,p},\ldots,f_{j,p},g_{i,p},\ldots,f_{i,p},g_{j,p},\ldots,f_{D,p},g_{D,p}) = P(f_{1,p},g_{1,p},\ldots,g_{i,p},f_{i,p},\ldots,f_{j,p},g_{j,p},\ldots,f_{D,p},g_{D,p}), \quad \text{(A4)}$$

for all $i,j,k=1,\ldots,D$. This is most easily done by drawing individual numbers from the same even probability distribution, i.e.,

$$P(f_{1,p},g_{1,p},\ldots,f_{j,p},g_{i,p},\ldots,f_{i,p},g_{j,p},\ldots,f_{D,p},g_{D,p}) = \prod_{n,m=1}^{D} P(f_{n,p})P(g_{n,p}), \quad \text{(A5)}$$

where $P(x)=P(-x)$. Normalizing the vector $(f_{1,p},g_{1,p},\ldots,f_{D,p},g_{D,p})$ such that $\Sigma_{i=1}^{D}|c_{n,p}|^2=1$ (for $p=1,\ldots,S$), does not affect the basic requirements (A3) and (A4).

Making use of the above properties of $P(f_1,g_1,\ldots,f_D,g_D)$, we find that

$$E(c_{m,p}^{*}c_{n,p}) = \delta_{m,n}E(|c_{m,p}|^2) = \delta_{m,n}E(|c|^2), \quad \text{(A6)}$$

where in the last equality we omitted the subscripts of $c_{m,p}$ to indicate that the expectation value does not depend on m or p. An expectation value of a product of two c^*'s and two c's can be written as

$$\begin{aligned}
E(c_{m,p}^{*}c_{n,p}c_{k,p'}c_{l,p'}^{*}) &= (1-\delta_{p,p'})\delta_{m,n}\delta_{k,l}E(|c_{m,p}|^2)E(|c_{m,p'}|^2) + \delta_{p,p'}\delta_{m,n}\delta_{k,l}(1-\delta_{mk})E(c_m^{*}c_m c_k c_k^{*}) \\
&\quad + \delta_{p,p'}\delta_{m,k}\delta_{n,l}(1-\delta_{m,n})E(c_m^{*}c_n c_m c_n^{*}) + \delta_{p,p'}\delta_{m,l}\delta_{n,k}(1-\delta_{m,n})E(c_m^{*}c_n c_n c_m^{*}) \\
&\quad + \delta_{p,p'}\delta_{m,l}\delta_{n,k}\delta_{m,n}E(c_m^{*}c_m c_m c_m^{*}) \\
&= (1-\delta_{p,p'})\delta_{m,n}\delta_{k,l}E(|c|^2)^2 + \delta_{p,p'}\delta_{m,n}\delta_{k,l}(1-\delta_{m,k})E(|c_{m,p}|^2|c_{k,p}|^2) \\
&\quad + \delta_{p,p'}\delta_{m,k}\delta_{n,l}(1-\delta_{m,n})E(|c_{m,p}|^2|c_{n,p}|^2) + \delta_{p,p'}\delta_{m,l}\delta_{n,k}(1-\delta_{m,n})E(c_{m,p}^{*}c_{n,p}c_{n,p}c_{m,p}^{*}) \\
&\quad + \delta_{p,p'}\delta_{m,l}\delta_{n,k}\delta_{m,n}E(|c_{m,p}|^4). \quad \text{(A7)}
\end{aligned}$$

Furthermore, for $m\neq n$ we have

$$\begin{aligned}
E(c_{m,p}^{*}c_{n,p}c_{n,p}c_{m,p}^{*}) &= E((f_{m,p}^2-2if_{m,p}g_{m,p}-g_{m,p}^2)(f_{n,p}^2+2if_{n,p}g_{n,p}-g_{n,p}^2)) \\
&= E(f_{m,p}^2f_{n,p}^2)+2iE(f_{m,p}^2f_{n,p}g_{n,p})-E(f_{m,p}^2g_{n,p}^2)-2iE(f_{m,p}g_{m,p}f_{n,p}^2)+4E(f_{m,p}f_{n,p}g_{m,p}g_{n,p}) \\
&\quad +2iE(f_{m,p}g_{m,p}g_{n,p}^2)-E(g_{m,p}^2f_{n,p}^2)-2iE(g_{m,p}^2f_{n,p}g_{n,p})+E(g_{m,p}^2g_{n,p}^2) \\
&= E(f_{m,p}^2f_{n,p}^2)-E(g_{m,p}^2f_{n,p}^2)-E(f_{m,p}^2g_{n,p}^2)+E(g_{m,p}^2g_{n,p}^2) \\
&= 0. \quad \text{(A8)}
\end{aligned}$$

By symmetry $E(|c_{m,p}|^2|c_{n,p}|^2)$ does not depend on m, n, or p, and the same holds for $E(|c_{m,p}|^4)$.

The fact that the vector $(c_{1,p},\ldots,c_{D,p})$ is normalized yields the identities

$$E\left(\sum_{n=1}^{D}|c_{n,p}|^2\right) = \sum_{n=1}^{D}E(|c_{n,p}|^2) = DE(|c|^2) = E(1) = 1 \quad \text{(A9)}$$

and

$$\begin{aligned}
&E\left(\left(\sum_{n=1}^{D}|c_{n,p}|^2\right)^2\right) \\
&= \sum_{m,n=1}^{D}E(|c_{n,p}|^2|c_{m,p}|^2) \\
&= \sum_{n=1}^{D}E(|c_{n,p}|^4) + \sum_{m,n=1}^{D}(1-\delta_{m,n})E(|c_n|^2|c_m|^2) \\
&= DE(|c|^4) + D(D-1)E(|c|^2|c'|^2) = E(1) = 1, \quad \text{(A10)}
\end{aligned}$$

where c and c' refer to two different complex random variables. Therefore, we have

$$E(|c|^2)=1/D \tag{A11}$$

and

$$E(|c|^2|c'|^2)=\frac{1-DE(|c|^4)}{D(D-1)}. \tag{A12}$$

Substitution into Eq. (A7) yields

$$\begin{aligned}E(c^*_{m,p}c_{n,p}c_{k,p'}c^*_{l,p'})&=(1-\delta_{p,p'})\delta_{m,n}\delta_{k,l}D^{-2}\\&+\delta_{p,p'}\frac{1-DE(|c|^4)}{D(D-1)}(\delta_{m,n}\delta_{k,l}(1-\delta_{m,k})\\&+\delta_{m,k}\delta_{n,l}(1-\delta_{m,n}))+\delta_{p,p'}\delta_{m,l}\delta_{n,k}\delta_{m,n}E(|c|^4),\end{aligned} \tag{A13}$$

and the final result for the variance reads

$$\begin{aligned}E(|\mathrm{Tr}\,RA|^2)=\frac{1}{S}\Bigg(&\frac{D-D^2E(|c|^4)}{D-1}\mathrm{Tr}\,A^\dagger A\\&+\frac{1-D^2E(|c|^4)}{D-1}|\mathrm{Tr}\,A|^2\\&+\frac{(D+1)D^2E(|c|^4)-2D}{D-1}\sum_{n=1}^{D}|A_{n,n}|^2\Bigg).\end{aligned} \tag{A14}$$

An expression for the fourth moment $E(|c|^4)$ cannot be derived from general properties of the probability distribution or normalization of random vector. We can only make progress by specifying the former explicitly. As an example we take a probability distribution such that for each realization p the random numbers $f_{n,p}$ and $g_{n,p}$ are distributed uniformly over the surface of a $2D$-dimensional sphere of radius 1. This probability distribution can be written as

$$\begin{aligned}&P(f_1,g_1,f_2,g_2,\ldots,f_D,g_D)\\&\quad\propto\delta(f_1^2+g_1^2+f_2^2+g_2^2+\cdots+f_D^2+g_D^2-1),\end{aligned} \tag{A15}$$

where we omitted the subscript p because it is irrelevant for what follows. The even moments of $|c_n|=(f_n^2+g_n^2)^{1/2}$ are defined by

$$E(|c|^{2M})=\frac{\int_{-\infty}^{\infty}(f_1^2+g_1^2)^M\delta(f_1^2+g_1^2+f_2^2+g_2^2+\cdots+f_D^2+g_D^2-1)df_1dg_1df_2dg_2\cdots df_Ddg_D}{\int_{-\infty}^{\infty}\delta(f_1^2+g_1^2+\cdots+f_D^2+g_D^2-1)df_1dg_1\cdots df_Ddg_D}. \tag{A16}$$

It is expedient to introduce an auxiliary integration variable X by

$$E(|c|^{2M})=\frac{\int_{-\infty}^{\infty}X^M\delta(f_1^2+g_1^2-X)\,\delta(f_2^2+g_2^2+\cdots+f_D^2+g_D^2-(1-X))dXdf_1dg_1df_2dg_2\cdots df_Ddg_D}{\int_{-\infty}^{\infty}\delta(f_1^2+g_1^2+\cdots+f_D^2+g_D^2-1)df_1dg_1\cdots df_Ddg_D}. \tag{A17}$$

We can perform the integration over X last and regard Eq. (A17) as the Mth moment of the variable X with respect to the probability distribution:

$$P(X)=\frac{\int_{-\infty}^{\infty}\delta(f_1^2+g_1^2-X)\,\delta(f_2^2+g_2^2+\cdots+f_D^2+g_D^2-(1-X))df_1dg_1df_2dg_2\cdots df_Ddg_D}{\int_{-\infty}^{\infty}\delta(f_1^2+g_1^2+\cdots+f_D^2+g_D^2-1)df_1dg_1\cdots df_Ddg_D}. \tag{A18}$$

The calculation of $P(X)$ amounts to computing integrals of the form

$$I_N(X)=\int_{-\infty}^{\infty}\delta\Bigg(\sum_{n=1}^{N}x_n^2-X\Bigg)dx_1dx_2\cdots dx_N. \tag{A19}$$

Changing to spherical coordinates, we have

$$\begin{aligned}I_N(X)&=\frac{2\pi^{N/2}}{\Gamma(N/2)}\int_0^\infty r^{N-1}\delta(r^2-X)dr\\&=\frac{\pi^{N/2}}{\Gamma(N/2)}X^{N/2-1}\theta(X),\end{aligned} \tag{A20}$$

yielding

$$P(X)=\frac{I_2(X)I_{2D-2}(1-X)}{I_{2D}(1)}$$
$$=(D-1)(1-X)^{D-2}\theta(X)\,\theta(1-X). \quad \text{(A21)}$$

The moments $E(|c|^{2M})$ are given by

$$E(|c|^{2M})=\int_{-\infty}^{\infty}X^M P(X)dX$$
$$=(D-1)\int_0^1 X^M(1-X)^{D-2}dX=\frac{\Gamma(D)\Gamma(1+M)}{\Gamma(D+M)}, \quad \text{(A22)}$$

and the values of interest to us are

$$E(|c|^0)=1,\ \ E(|c|^2)=\frac{1}{D},\ \ E(|c|^4)=\frac{2}{D(D+1)}, \quad \text{(A23)}$$

where the first two results provide some check on the procedure used. Substituting Eq. (A23) into Eq. (A14) yields

$$E(|\mathrm{Tr}\,RA|^2)=\frac{D\,\mathrm{Tr}\,A^\dagger A-|\mathrm{Tr}\,A|^2}{S(D+1)}. \quad \text{(A24)}$$

APPENDIX B: ERROR BOUNDS

Here we prove that the difference between the eigenvalues of the Hermitian matrix $A+B$ and those obtained from the approximate time-evolution $\exp(zA/2)\exp(zB)\exp(zA/2)$ $(z=-i\tau,-\tau)$ is bounded by τ^2. In the following we assume A and B are Hermitian matrices and take τ, a real, nonnegative number. We start with the imaginary-time case.

We define the difference $R(\tau)$ by

$$R(\tau)\equiv e^{\tau(A+B)}-e^{\tau A/2}e^{\tau B}e^{\tau A/2}$$
$$=\frac{1}{4}\int_0^\tau d\lambda\int_0^\lambda d\mu\int_0^\mu d\nu e^{\lambda A/2}e^{\lambda B}\{e^{-\nu B}[2B,[A,B]]e^{\nu B}$$
$$+e^{\nu A/2}[A,[A,B]]e^{-\nu A/2}\}e^{\lambda A/2}e^{(\tau-\lambda)(A+B)}, \quad \text{(B1)}$$

a well-known result [24]. We have [26]

$$\|R(\tau)\|\le\frac{1}{4}\left\|\int_0^\tau d\lambda\int_0^\lambda d\mu\int_0^\mu d\nu e^{\lambda A/2}e^{(\lambda-\nu)B}[2B,[A,B]]e^{\nu B}e^{\lambda A/2}e^{(\tau-\lambda)(A+B)}\right\|$$
$$+\frac{1}{4}\left\|\int_0^\tau d\lambda\int_0^\lambda d\mu\int_0^\mu d\nu e^{\lambda A/2}e^{\lambda B}e^{\nu A/2}[A,[A,B]]e^{(\lambda-\nu)A/2}e^{(\tau-\lambda)(A+B)}\right\|$$
$$\le\frac{1}{4}\int_0^\tau d\lambda\int_0^\lambda d\mu\int_0^\mu d\nu e^{\lambda\|A\|/2}e^{(\lambda-\nu)\|B\|}\|[2B,[A,B]]\|e^{\nu\|B\|}e^{\lambda\|A\|/2}e^{(\tau-\lambda)(\|A\|+\|B\|)}$$
$$+\frac{1}{4}\int_0^\tau d\lambda\int_0^\lambda d\mu\int_0^\mu d\nu e^{\lambda\|A\|/2}e^{\lambda\|B\|}e^{\nu\|A\|/2}\|[A,[A,B]]\|e^{(\lambda-\nu)\|A\|/2}e^{(\tau-\lambda)(\|A\|+\|B\|)}$$
$$=\frac{1}{24}\tau^3e^{\tau(\|A\|+\|B\|)}(\|[A,[A,B]]\|+\|[2B,[A,B]]\|), \quad \text{(B2)}$$

and

$$\|R(-\tau)\|\le\frac{1}{4}\left\|\int_0^{-\tau}d\lambda\int_0^\lambda d\mu\int_0^\mu d\nu e^{\lambda A/2}e^{(\lambda-\nu)B}[2B,[A,B]]e^{\nu B}e^{\lambda A/2}e^{(-\tau-\lambda)(A+B)}\right\|$$
$$+\frac{1}{4}\left\|\int_0^{-\tau}d\lambda\int_0^\lambda d\mu\int_0^\mu d\nu e^{\lambda A/2}e^{\lambda B}e^{\nu A/2}[A,[A,B]]e^{(\lambda-\nu)A/2}e^{(-\tau-\lambda)(A+B)}\right\|$$
$$=\frac{1}{4}\left\|\int_0^\tau d\lambda\int_0^\lambda d\mu\int_0^\mu d\nu e^{-\lambda A/2}e^{(-\lambda+\nu)B}[2B,[A,B]]e^{-\nu B}e^{-\lambda A/2}e^{(-\tau+\lambda)(A+B)}\right\|$$
$$+\frac{1}{4}\left\|\int_0^\tau d\lambda\int_0^\lambda d\mu\int_0^\mu d\nu e^{-\lambda A/2}e^{-\lambda B}e^{-\nu A/2}[A,[A,B]]e^{(-\lambda+\nu)A/2}e^{(-\tau+\lambda)(A+B)}\right\|$$
$$\le\frac{1}{4}\int_0^\tau d\lambda\int_0^\lambda d\mu\int_0^\mu d\nu e^{\lambda\|A\|/2}e^{(\lambda-\nu)\|B\|}\|[2B,[A,B]]\|e^{\nu\|B\|}e^{\lambda\|A\|/2}e^{(\tau-\lambda)(\|A\|+\|B\|)}$$
$$+\frac{1}{4}\int_0^\tau d\lambda\int_0^\lambda d\mu\int_0^\mu d\nu e^{\lambda\|A\|/2}e^{\lambda\|B\|}e^{\nu\|A\|/2}\|[A,[A,B]]\|e^{(\lambda-\nu)\|A\|/2}e^{(\tau-\lambda)(\|A\|+\|B\|)}$$
$$=\frac{1}{24}\tau^3e^{\tau(\|A\|+\|B\|)}(\|[A,[A,B]]\|+\|[2B,[A,B]]\|). \quad \text{(B3)}$$

Hence the bound in $R(\tau)$ does not depend on the sign of τ so that we can write

$$\|R(\tau)\| \leq s|\tau|^3 e^{|\tau|(\|A\|+\|B\|)}, \tag{B4}$$

where

$$s \equiv \frac{1}{24}\|[A,[A,B]]\| + \|[2B,[A,B]]\|. \tag{B5}$$

For real τ we have

$$e^{\tau A/2} e^{\tau B} e^{\tau A/2} \equiv e^{\tau C(\tau)}, \tag{B6}$$

where $C(\tau)$ is Hermitian. Clearly we have

$$e^{\tau(A+B)} - e^{\tau C(\tau)} = R(\tau). \tag{B7}$$

We already have an upper bound on $R(\tau)$, and now want to use this knowledge to put an upper bound on the difference in eigenvalues of $C(\tau)$ and $A+B$. In general, for two Hermitian matrices U and V with eigenvalues $\{u_n\}$ and $\{v_n\}$, respectively, both sets sorted in nondecreasing order, we have [2]

$$|u_n - v_n| \leq \|U-V\|, \quad \forall\, n. \tag{B8}$$

Denoting the eigenvalues of $A+B$ and $C(\tau)$ by $x_n(0)$ and $x_n(\tau)$, respectively, combining Eqs. (B4) and (B8) yields

$$|e^{\tau x_n(0)} - e^{\tau x_n(\tau)}| \leq s|\tau|^3 e^{|\tau|(\|A\|+\|B\|)}. \tag{B9}$$

To find an upper bound on $|x_n(0) - x_n(\tau)|$ we first assume that $x_n(0) \leq x_n(\tau)$ and take $\tau \geq 0$. It follows from Eq. (B9) that

$$e^{\tau(x_n(\tau)-x_n(0))} - 1 \leq s\tau^3 e^{\tau(\|A\|+\|B\|)-\tau x_n(0)}. \tag{B10}$$

For $x \geq 0$, $e^x - 1 \geq x$ and we have $-x_n(0) \leq \|A+B\| \leq \|A\| + \|B\|$. Hence we find

$$x_n(\tau) - x_n(0) \leq s\tau^2 e^{2\tau(\|A\|+\|B\|)}. \tag{B11}$$

An upper bound on the difference in the eigenvalues between $C(\tau)$ and $A+B$ can equally well be derived by considering the inverse of the exact and approximate time-evolution operator (B6). This is useful for the case $x_n(0) > x_n(\tau)$: Instead of using Eq. (B7) we start from $\exp(-\tau(A+B)) - \exp(-\tau C(-\tau)) = R(-\tau)$ $(\tau \geq 0)$. Note that the set of eigenvalues of a matrix and its inverse are the same and that the matrices we are considering here, i.e., matrix exponentials, are nonsingular. Making use of Eq. (B4) for $R(-\tau)$ gives

$$|e^{-\tau x_n(0)} - e^{-\tau x_n(\tau)}| \leq s|\tau|^3 e^{|\tau|(\|A\|+\|B\|)}, \tag{B12}$$

and proceeding as before we find

$$\tau(x_n(0) - x_n(\tau)) \leq e^{\tau(x_n(0)-x_n(\tau))} - 1 \leq s\tau^3 e^{2\tau(\|A\|+\|B\|)}. \tag{B13}$$

Putting the two cases together, we finally have

$$|x_n(\tau) - x_n(0)| \leq s\tau^2 e^{2\tau(\|A\|+\|B\|)}. \tag{B14}$$

Clearly Eq. (B14) proves that the differences in the eigenvalues of $A+B$ and $C(\tau)$ vanish as τ^2.

We now consider the case of the real-time algorithm ($z = -i\tau$). For Hermitian matrices A and B the matrix exponentials are unitary matrices, and hence their norm equals 1. This simplifies the derivation of the upperbound on $R(-i\tau)$. One finds [20]

$$\|R(-i\tau)\|_E \leq s|\tau|^3, \tag{B15}$$

where $\|A\|_E^2 \equiv \mathrm{Tr}\, A^\dagger A$ denotes the Euclidean norm of the matrix A [2]. In general the eigenvalues of a unitary matrix are complex valued, and therefore the strategy adopted above to use the bound on $R(\tau)$ to set a bound on the difference of the eigenvalues no longer works. Instead we invoke the Wielandt-Hoffman theorem [27]:

If U and V are *normal matrices with eigenvalues u_i and v_i respectively, then there exists a suitable rearrangement (a permutation ϱ of the numbers* $1, \ldots, n$*) of the eigenvalues so that*

$$\sum_{j=1}^{N} |u_j - v_{\varrho(j)}|^2 \leq \|U-V\|_E^2. \tag{B16}$$

Let U and V denote the exact and approximate real-time evolution operators respectively. The eigenvalues of $A+B$ and $C(\tau)$ are $x_n(0)$ and $x_n(\tau)$, respectively. All the x_n's and $x_n(\tau)$'s are real numbers. According to the Wielandt-Hoffman theorem

$$\sum_{j=1}^{N} |e^{i\tau x_j(0)} - e^{i\tau y_j(\tau)}|^2 \leq \|R(-i\tau)\|_E^2 \leq s^2\tau^6. \tag{B17}$$

where $y_j(\tau) = x_{\varrho(j)}(\tau)$, ϱ being the permutation such that inequality (B17) is satisfied. We see that Eq. (B17) only depends on $(\tau x_j(0) \bmod 2\pi)$ and $(\tau y_j(\tau) \bmod 2\pi)$, but so does the DOS [see Eq. (16)]. Since inequality (B17) and the DOS only depend on these ''angles'' modulo 2π, there is no loss of generality if we make the choice

$$0 \leq |\tau(x_j(0) - y_j(\tau))| \leq \pi. \tag{B18}$$

Rewriting the sum in Eq. (B17), we have

$$\sum_{j=1}^{N} |e^{i\tau x_j(0)} - e^{i\tau y_j(\tau)}|^2 = \sum_{j=1}^{N} \{2 - 2\cos[\tau(x_j(0) - y_j(\tau))]\} = 4\sum_{j=1}^{N} \sin^2[\tau/2\,(x_j(0) - y_j(\tau))]. \tag{B19}$$

As we have

$$\sin^2 x \leq \frac{4x^2}{\pi^2} \quad \text{for} \quad 0 \leq |x| \leq \pi/2, \tag{B20}$$

the restriction Eq. (B18) allows us to write

$$\sum_{j=1}^{N} (x_j(0) - y_j(\tau))^2 \leq \frac{\pi^2 s^2}{4}\tau^4, \tag{B21}$$

implying

$$|x_j(0)-y_j(\tau)|\leqslant \frac{\pi s}{2}\tau^2. \tag{B22}$$

In summary, we have shown that in the real-time case there exists a permutation of the approximate eigenvalues such that the difference with the exact ones vanishes as τ^2.

Finally we note that both upper bounds (B22) and (B14) hold for arbitrary Hermitian matrices A and B and are therefore rather weak. Except for the fact that they provide a sound theoretical justification for the real- and imaginary time method, they are of little practical value.

[1] G. D. Mahan, *Many-Particle Physics* (Plenum Press, New York, 1981).
[2] J. H. Wilkinson, *The Algebraic Eigenvalue Problem* (Clarendon Press, Oxford, 1965).
[3] G. H. Golub and C. F. Van Loan, *Matrix Computations* (John Hopkins University Press, Baltimore, MD, 1983).
[4] R. Alben, M. Blume, H. Krakauer, and L. Schwartz, Phys. Rev. B **12**, 4090 (1975).
[5] M. D. Feit, J. A. Fleck, and A. Steiger, J. Comput. Phys. **47**, 412 (1982).
[6] H. De Raedt and P. de Vries, Z. Phys. B: Condens. Matter **77**, 243 (1989).
[7] T. Kawarabayashi and T. Ohtsuki, Phys. Rev. B **53**, 6975 (1996).
[8] T. Ohtsuki and T. Kawarabayashi, J. Phys. Soc. Jpn. **66**, 314 (1997).
[9] T. Iitaka, S. Nomura, H. Hirayama, X. Zhao, Y. Aoyagi, and T. Sugano, Phys. Rev. E **56**, 1222 (1997).
[10] S. Nomura, T. Iitaka, X. Zhao, T. Sugano, and Y. Aoyagi, Phys. Rev. B **56**, 4348 (1997).
[11] S. Nomura, T. Iitaka, X. Zhao, T. Sugano, and Y. Aoyagi, Phys. Rev. B **59**, 10 309 (1999).
[12] T. Iitaka and T. Ebisuzaki, Phys. Rev. E **60**, 1178 (1999).
[13] T. Iitaka and T. Ebisuzaki, Microelectron. Eng. **47**, 321 (1999).
[14] T. Iitaka and T. Ebisuzaki, Phys. Rev. E **61**, 3314 (2000).
[15] P. de Vries and H. De Raedt, Phys. Rev. B **47**, 7929 (1993).
[16] H. De Raedt, A. Hams, K. Michielsen, S. Miyashita, and K. Saito, Prog. Theor. Phys. **138**, 489 (2000).
[17] D. S. Abrams and S. Lloyd, Phys. Rev. Lett. **83**, 5162 (1999).
[18] G. R. Grimmet and D. R. Stirzaker, *Probability and Random Processes* (Clarendon, Oxford, 1992).
[19] E. Lieb, T. Schultz, and D. C. Mattis, Ann. Phys. (N.Y.) **16**, 407 (1961).
[20] H. De Raedt, Comput. Phys. Rep. **7**, 1 (1987).
[21] M. Suzuki, S. Miyashita, and A. Kuroda, Prog. Theor. Phys. **58**, 1377 (1977).
[22] $\|X\|$ denotes the spectral norm of the matrix X; see *The Algebraic Eigenvalue Problem* (Ref. [2]) and *Matrix Computations* (Ref. [3]).
[23] H. De Raedt and B. De Raedt, Phys. Rev. A **28**, 3575 (1983).
[24] M. Suzuki, J. Math. Phys. **26**, 601 (1985).
[25] H. De Raedt and K. Michielsen, Comput. Phys. **8**, 600 (1994).
[26] M. Suzuki, J. Math. Phys. **61**, 3015 (1995).
[27] A. J. Hoffman and H. W. Wielandt, Duke Math. J. **20**, 37 (1953).